Generating Second Order (Co)homological Information within AT-Model Context

Pedro Real[1], Helena Molina-Abril[1], Fernando Díaz del Río[1], and Darian Onchis[2,3]

[1] H.T.S. Informatics' Engineering, University of Seville, Seville, Spain
{real,habril}@us.es, fdiaz@atc.us.es
[2] Faculty of Mathematics, University of Vienna, Vienna, Austria
darian.onchis@univie.ac.at
[3] Faculty of Mathematics and Computer Science, West University of Timisoara, Timişoara, Romania

Abstract. In this paper we design a new family of relations between (co)homology classes, working with coefficients in a field and starting from an AT-model (Algebraic Topological Model) $AT(C)$ of a finite cell complex C These relations are induced by elementary relations of type "to be in the (co)boundary of" between cells. This high-order connectivity information is embedded into a graph-based representation model, called *Second Order AT-Region-Incidence Graph (or AT-RIG)* of C. This graph, having as nodes the different homology classes of C, is in turn, computed from two generalized abstract cell complexes, called *primal and dual AT-segmentations* of C. The respective cells of these two complexes are connected regions (set of cells) of the original cell complex C, which are specified by the integral operator of $AT(C)$. In this work in progress, we successfully use this model (a) in experiments for discriminating topologically different 3D digital objects, having the same Euler characteristic and (b) in designing a parallel algorithm for computing potentially significant (co)homological information of 3D digital objects.

Keywords: Cell complex · Algebraic-topological model
Homology computation · Primal and dual AT-segmentation
AT-model region-incidence-graph · nD digital object

1 Introduction

(Co)homology (see for instance [33]) provides valuable information about topological spaces, by observing sets that intuitively have no (co)boundary, but are

This work has been supported by the Spanish research projects MTM2016-81030-P (AEI/FEDER, UE) and TEC2012-37868-C04-02, and by the VPPI of the University of Seville. Darian Onchis gratefully acknowledges the support of the Austrian Science Fund FWF-P27516.

on the (co)boundary of other sets. These sets are representative (co)cycles of a (co)homology hole, seen as an equivalence class. Algebraic (co)homological information with coefficients in a field could be defined as the set of processed and structured linear algebraic data describing in some sense its (co)homology classes and the relations between them. We talk about homology and cohomology information as a whole due to the fact that homology and cohomology classes are measured using different strategies (delineating or cutting holes) for detecting homological holes over the initial topological data. A simple example of (co)homology information is provided by the numerical topological invariants called Betti numbers. For instance, if X is a cell complex embedded in $\mathbb{R}^3$, Betti numbers β_0, β_1 and β_2 respectively measure the number of different connected components, tunnels and cavities of X.

Roughly speaking, (co)homotopy holes of objects (those related to delineating or cutting generalized "parametrized and oriented closed curves") are theoretically attainable from homology's ones [23], but these methods have an enormous complexity in time and space [4]. An easier relation between homology and homotopy is given by the Euler characteristic (see [1]), defined in local terms as the alternate sum of the number of cells in each dimension. This number is the most simple example of homotopy invariant, that can also be obtained from the global homological information provided by the Betti numbers.

Now, (co)homology information of X is not reduced in general to that provided by Betti numbers. For example, a torus T and a three-dimensional sphere with two handles S have the same Betti numbers (and, consequently the same Euler characteristic) but they are not (co)homologically equivalents. The two tunnels of T are related to its cavity in a much more "stronger" way that the tunnels of S are with regards to the corresponding cavity.

We progress here in discovering the homotopy nature of homology, by creating two (non-unique) abstract cell complexes, called *primal and dual AT-segmentations*, both with significantly smaller number of cells than the original geometric cell complex C and from which it is possible to detect topological relationships between (co)homology classes of C with coefficient in a field $\mathbb{F}$. We construct the primal and dual segmentation with the help of an algebraic-topological model $AT(C)$ of C (or AT-model for short) [17,18,34,35]. Using the bounding functions of a primal and dual AT-segmentations and the relationship between cells "to be in the boundary of", we are finally able to compute a graph-based model $\mathcal{P}(AT(C))$, called *AT-model Region-Incidence-Graph* (or, *AT-RIG*, for short), whose nodes are the different homology classes of C.

We successfully use this technique in a set of experiments for discriminating topologically different 3D digital objects with the same Euler characteristic. We also use this modus operandi in designing a parallel algorithm for computing potential high-order homology statistics for a 3D digital objects. In a near future, we intend to study the corresponding degrees of independence with regards the AT-model chosen and of homology and homotopy invariances of an AT-RIG.

1.1 Related Works

Focusing on homotopy representation models of digital objects and images, there are numerous works that arise from sources of digital topology [2,21,25], continuous or cellular topology [9,20,26] and nD shape search with three clearly differentiated notions: Reeb graphs [5,13], skeletons [6,36,41] and boundary representations [3,16,28]. Relative to the intermediary step of homological computation of cell complexes, there is plenty of literature based on a pure algebraic perspective devoted to this issue. The classical method is based on the diagonalization of cell-incidence matrices to Smith normal form (SNF) [33]. Some advances in the computation of the SNF have been achieved [10], but the most successful approaches consist of reducing the number of cells in the complex using discrete-vector-field dynamics (Discrete Morse theory [12]) before computing the SNF for the small resulting cell complex (see, for instance, [7,14,19,22,32,35,39,40]). This paper goes beyond homological computation and designs (sequential and parallel) algorithms for computing a new graph-based representation that allows to discriminate homologically different geometric objects embedded in $\mathbb{R}^n$ having the same Betti numbers. In this sense, AT-segmentation theory extend and greatly improve both the algebraic model called Algebraic-Topological model [17,18,34,35,37] and the combinatorial model called Homological Spanning Forest (HSF, for short) [8,30,31,38] in this search of topological representations within digital image context.

2 Cell Complexes and Algebraic-Topological Models

We work in this paper with cell complex representations (composed of cells and bounding relations between them), that allow to model, for example, not only an n-dimensional digital object at sub-n-xel level but also significant algebraic (co)homological information (with coefficient in a field $\mathbb{F}$).

First at all, we provide a slightly modified version of the classical abstract cell complex notion (see [24] for a survey).

We say that $\mathsf{C} = (C, B, dms)$ is an *abstract cell complex (or ACC, for short)* if:

- $C = \{C_q\}_{q \in \mathbb{N} \cup \{0\}}$ is a finite set with a gradation $dms : C \to \mathbb{N} \bigcup \{0\}$ defined by $dms(c) = q$ for $c \in C_q$;
- $B : C \times C \to \mathbb{N} \cup \{0\}$ is a map such that satisfies the following condition: $B(c, c') \neq 0$ implies $c \in C_{q-1}$, $c' \in C_q$.

We refer to the elements of C as cells and to $B(c, c')$ as the bounding function of the ACC C applied to the couple (c, c'). If we extend the bounding function of the ACC in an antisymmetric and transitively way, we recover the classical notion of ACC.

The *connectivity-graph* $G(C, B, dms) = (V, E)$ of an abstract cell complex (C, B, dms) is the graph whose set of nodes is C and an edge $\{c, c'\} \in E$ if $B(c, c')$ or $B(c', c)$ is different from zero.

Now, let us define the (algebraic) notion of geometric cell complex. We say that $\mathsf{C} = (C, \kappa, dms)$ is a *Lefschetz complex* [27] if:

- $C = \{C_q\}_{q \in \mathbb{N} \cup \{0\}}$ is a finite set with a gradation $dms : C \to \mathbb{N} \bigcup \{0\}$ defined by $dms(c) = q$ for $c \in C_q$;
- $\kappa : C \times C \to \mathbb{F}$ is a map such that $\kappa(c, c') \neq 0$ implies $c \in C_{q-1}$, $c' \in C_q$. For any $c, c'' \in C$ we have $\sum_{c' \in C} \kappa(c, c')\kappa(c', c'') = 0$.

We refer to the elements of C as cells and to $\kappa(x, y)$ as the incidence coefficient of x, y.

In fact, an equivalent definition of a Lefschetz complex is that of a free chain complex $(\mathbb{F}[C], \partial_C)$ with *boundary* $\partial_C : \mathbb{F}[C] \to \mathbb{F}[C]$ defined on generators by $\partial_C(c) = \sum_{c' \in C} \kappa(c', c)c'$. Its *coboundary* $\delta_C : \mathbb{F}[C] \to \mathbb{F}[C]$ is defined on generators by $\delta_C(c) = \sum_{c' \in C} \kappa(c, c')c'$. The Lefschetz homology (resp. cohomology) of (C, κ, dms), denoted $H(\mathsf{C}, \partial_C)$ (resp. $H(\mathsf{C}, \delta_C)$) is the homology of the chain complex $(\mathbb{F}[C], \partial)$ (resp. $(\mathbb{F}[C], \delta)$). We are interested here in Lefschetz complexes satisfying that for any $c, c' \in C$ the incidence coefficient $\kappa(c, c')$ is either zero or ± 1 of $\mathbb{F}$. These structures are simply called here *geometric cell complexes*. The identity function $1_C : C \to C$ is defined by $1_C(c) = c$, $\forall c \in C$. Associated to a geometric cell complex (C, κ, dms), there is a bounding function $B : C \times C \to \mathbb{N} \cup \{0\}$ defined by $B(c, c') = 1$ if $\kappa(c, c') \neq 0$ and $B(c, c') = 0$ in the rest of cases. If $c \in C$ and R is a set of cells of (C, κ, dms), we define the bounding function $B(c, R) = \sum_{c' \in R} B(c, c')$ (resp. $B(R, c) = \sum_{c' \in R} B(c, c')$).

From now on, we use the triplet (C, ∂, dms) for denoting a geometric cell complex. We use the notation $c' \in f$, being $f \in \mathbb{F}[C]$, for indicating that the cell c' is involved as a non-null summand in this linear combination.

It is straightforward to specify geometric cell complexes structures modeling n-dimensional digital images at sub-n-xel level. In fact, we are mainly interested in running the designed algorithms for "cellularizations" of digital objects and images, in order to progress in topological acuity and representation within digital image context.

Now, we are able to define an *algebraic-topological model* (or AT-model, for short) (C, ∂, ϕ, dms) of a geometric cell complex (C, ∂, dms) (see [17]). The homomorphism $\phi : \mathbb{F}[C_q] \to \mathbb{F}[C_{q+1}]$, called *integral operator*, satisfies the following three conditions: (a) $\phi\phi = 0$; (b) $\partial\phi\partial = \partial$; (c) $\phi\partial\phi = \phi$. From this data, we can construct an explicit homology equivalence between the chain complex $(\mathbb{F}[C], \partial)$ and a free chain complex with null differential (which, obviously, is isomorphic to the homology $H(\mathsf{C}, \partial)$). The germ idea of the AT-model comes back to the original notion of chain contraction exhaustively used by Samuel Eilenberg and Saunder Mac Lane in their works of homological computation (see, for example, [11]) in the fifties of the twentieth century.

3 AT-Segmentations

In this section and with the help of an AT-model (C, ∂, ϕ, dms), we construct two special partitions of C into connected regions from which it is possible to compute "strong" topological relations between homology classes, derived from the elementary relation "to be in the boundary of". From now on, we work with $\mathbb{F} = \mathbb{Z}_2$, in order to avoid the use of signs in the AT-model construction.

Let us emphasize that all the study done here can be correctly developed for any ground field.

Some terminology relative to primal regions of the primal AT-segmentation we want to construct is necessary. The dimension of a primal region R composed by cells of C of dimension t $(0 \leq t \leq n-1)$ and, possibly, of dimension $t+1$ is $dim^{pr}(R) = (t, t+1)$. Its criticality number $crt(R)$ is given by the difference between the number of t-cells and $(t+1)$-cells. All the regions of a primal AT-segmentation have criticality number greater or equal to zero. A primal region R with $crt(R) > 0$ is called *homologically essential*. If $crt(R) = 0$ is called *homologically inessential*.

Algorithm 1 uses as input a filtration of the geometric cell complex C. It is possible to design an algorithm for computing a primal AT-segmentation independent of this restriction. Such algorithm is based on the construction of hierarchical "spanning forests" within the global connectivity graph of C as ACC. There is no space here to address this question in detail. The reference [37] can be of help in the planning of such algorithm.

Figure 1 shows a primal AT-segmentation over an ACC version $Cell(O)$ of a 2D digital object.

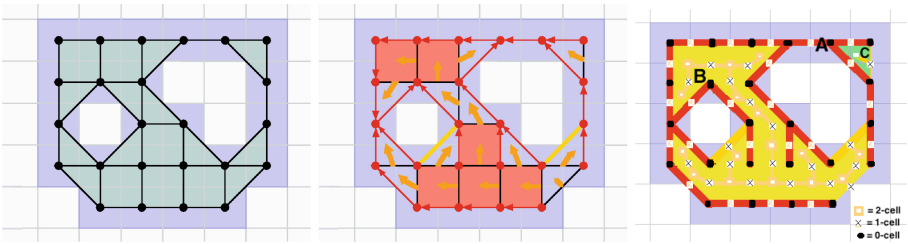

Fig. 1. (Left) ROI consisting of the set of black pixels. The implicit cellularization of the ROI -using 8-adjacency and being the 0-cells the square physical pixels- is superimposed. (Center) Vectors of cracks involved in the AT-model construction of Algorithm 1 are highlighted. (Right) The associated AT-segmentation of the ROI. There are three regions. Region A is drawn in red and is composed by all the 24 (N_0^A) 0-cells and 23 (N_1^A) 1-cells (a subdivision of the spanning tree of the 0-cells). Region B is drawn in yellow and is composed by 18 (N_1^B) 1-cells and 16 (N_2^B) 2-cells. Region C is drawn in green and its tree has one 1-cell and one 2-cell (thus, it is inessential). Regions A and B are homologically essential, due to the fact that $crt(R) = N_i^R - N_{i+1}^R = 1 > 0$, for $(R, i) = \{(A, 0), (B, 1)\}$. In fact, A detects one 0-dimensional homology class and B two 1-dimensional holes. (Color figure online)

Let us note that the connectivity graph of regions of the primal AT-segmentation $HS^{pr}(\mathsf{C})$ is not necessarily a tree. For each critical cell $e_q^{d_q}$, $(1 \leq q \leq m)$ its corresponding primal segmentation region $\mathcal{S}_\ell^{pr}(e_q^{d_q})$ of dimension (d_q, d_q+1) has a criticality number $crt(\mathcal{S}_\ell^{pr}(e_q^{d_q}))$ greater than zero. The rest of the primal segmentation regions have a criticality number equal to zero.

Algorithm 1. [primal AT-segmentation]

Input: A geometric cell complex $\mathsf{C} := \{C, \partial, dms\}$. C is a list with all the cells of C ordered by increasing dimension $c_1^0, \ldots c_{\ell_1}^0,\ c_1^1,\ \ldots,\ c_{\ell_2}^1,\ \ldots, c_1^n, \ldots, c_{\ell_n}^n$. Here, $dms(c_j^k) = k$, $\forall k, j$ and $\sum_{1\leq q\leq n} \ell_q = \ell$. Let us also use the cell ordering $c_j^k = c_{j+\sum_{q<k}\ell_q}$. The boundary operator $\partial_{|\mathbb{Z}[c_1,\ldots,c_i]}$ is denoted by ∂_i.

$\mathcal{H}_0^\partial \leftarrow \emptyset$; $\mathcal{K}_0^\phi \leftarrow \emptyset$; $\mathcal{J}_0^\phi \leftarrow \emptyset$; $\mathcal{S}_0^{pr} \leftarrow \emptyset$;
for $k = 0$ to n **do**
  for $j = 1$ to ℓ_k **do**
    $i \leftarrow j + \sum_{q<k} \ell_q$;
    $\phi_{i-1}(c_i) \leftarrow 0$;
    $\mathcal{R}_i \leftarrow \{c_i\}$;
    $\mathcal{S}_i^{pr} \leftarrow \mathcal{S}_{i-1}^{pr} \cup \{R_i\}$. Let us denote by $\mathcal{S}_i^{pr}(c_q)$ the region of $\mathcal{S}_i^{pr}$ containing the cell c_q $(1 \leq q \leq i)$. In this way, $\mathcal{S}_i^{pr}$ is handled as the union $\bigcup_{1\leq q\leq i}\{\mathcal{S}_i^{pr}(c_q)\}$.
    $Bnd_i \leftarrow \{e \in \partial_i(c_i)\}$; ▷ Boundary of the current cell
    $\bar{c}_i \leftarrow c_i + \phi_{i-1}\partial_i(c_i)$; ▷ Potential cycle associated to c_i
    $\overline{Bnd_i} \leftarrow \{e \in \partial_i(\bar{c}_i)\}$; ▷ Algebraic boundary of $\bar{c}_i$
    $\widetilde{Bnd_i} \leftarrow \{e \in (1_C + \partial_i\phi_{i-1})(c),\ \text{for some } c \in Bnd_i\}$; ▷ Combinatorial boundary of $\bar{c}_i$
    $\mathcal{N}_i \leftarrow \{e \in Bnd_i \colon dim^{pr}(S_i^{pr}(e)) = (dms(c_i) - 1, dms(c_i)) \wedge crt(S_i^{pr}(e)) = 0\}$; ▷ Homologically inessential regions in the boundary of c_i
    $\mathcal{H}_i^\partial \leftarrow H_{i-1}^\partial \bigcup\{\bar{c}_i\}$; $\mathcal{K}_i^\phi \leftarrow \mathcal{K}_{i-1}^\phi \bigcup\{c_i\}$; $\mathcal{J}_i^\phi \leftarrow \mathcal{J}_{i-1}^\phi \bigcup\{c_i\}$; ▷ Homology generators, combinatorial kernel, critical cells
    if $\partial_i(\bar{c}_i) == 0$ **then** ▷ Equivalent to $\overline{Bnd_i} == \emptyset$
      for $r = 1$ to i **do**
        $\phi_i(c_r) \leftarrow \phi_{i-1}(c_r)$;
    else ▷ In case in which c_i does not generate a cycle
      $\overline{\mathcal{J}}_i \leftarrow \overline{Bnd_i} \bigcap \mathcal{J}_i^\phi$
      $\tilde{\mathcal{J}}_i \leftarrow \widetilde{Bnd_i} \bigcap \mathcal{J}_i^\phi$
      $\mathcal{S}_i^{pr}(c_i) \leftarrow \mathcal{S}_i^{pr}(c_i) \bigcup_{e\in\tilde{\mathcal{J}}_i\cup\mathcal{N}_i} \mathcal{S}_i^{pr}(e)$; ▷ Updating the primal partition
      for $e \in \tilde{\mathcal{J}}_i \cup \mathcal{N}_i$ **do**
        $\mathcal{S}_i^{pr}(e) \leftarrow \mathcal{S}_i^{pr}(c_i)$;
      Choose one of the cells $\mathbf{e} \in \overline{\mathcal{J}}_i$ ▷ Updating AT-model
      $\tilde{\phi}(\mathbf{e}) \leftarrow c_i$;
      $\tilde{\phi}(c) \leftarrow 0$ for each $c \in \mathcal{K}_{i-1}^\phi \setminus \{\mathbf{e}\}$;
      $\bar{\mathbf{e}} \leftarrow \mathbf{e} + \phi_{i-1}\partial_i(\mathbf{e})$;
      for $q = 1$ to $i - 1$ **do**
        $\phi_i(c_q) \leftarrow (\phi_{i-1} + (id_{\mathsf{C}_i} - \phi_{i-1}\partial_{i-1})\tilde{\phi}(id_{\mathsf{C}_i} - \partial_{i-1}\phi_{i-1}))(c_q)$, $\forall c_q \in \mathsf{C}_i$
      $\mathcal{H}_i^\partial \leftarrow \mathcal{H}_i^\partial \setminus \{\bar{\mathbf{e}}, \bar{c}_i\}$; ▷ Updating homology generators
      $\mathcal{K}_i^\phi \leftarrow \mathcal{K}_i^\phi \setminus \{\mathbf{e}\}$; ▷ Updating combinatorial homology kernel
      $\mathcal{J}_i^\phi \leftarrow \mathcal{J}_i^\phi \setminus \{\mathbf{e}, c_i\}$; ▷ Updating set of critical cells
$B^{pr}[\mathsf{C}](R, R') \leftarrow \#\{c' \in R' \colon dms(c') = t \wedge B(R, c') = \sum_{c\in R} B(c, c') \neq 0\}$
$\forall R, R' \in \mathcal{S}_\ell^{pr}$, with $dim^{pr}(R) = (t-1, t)$ and $dim^{pr}(R') = (t, t+1)$ $(1 \leq t \leq n)$.
▷ Specifying primal AT-segmentation bounding function

Output:

- An AT-model $(C, \partial_\ell, \phi_\ell, dms)$ and a combinatorial basis (set of *critical cells*) specified by $\mathcal{J}_\ell^\phi$ and ordered by increasing dimension $\{e_1^{d_1}, \ldots, e_m^{d_m}\}$ (with $dms(e_q^{d_q}) = d_q$, $1 \leq q \leq m$) for the homology $H(\mathsf{C}, \phi)$ given by $\mathcal{H}_\ell^\phi$.
- An abstract cell complex $HS^{pr}(\mathsf{C})$, called *primal AT-segmentation of* C, whose set of cells is the partition in regions $\mathcal{S}_\ell^{pr}$ of C and its bounding function is $B^{pr}[\mathsf{C}]$.

From this output, it is possible to define a dual AT-segmentation $HS^{dl}(\mathsf{C})$ in this simple manner:

- **[Initial dual AT-partition].** We consider as initial dual AT-partition $\overline{\mathcal{S}}_\ell^{dl}$ a refinement of the primal segmentation partition $\mathcal{S}_\ell^{pr}$, in which each critical cell (as sets formed by one element) is considered as a new region of the partition. Let us note that all the regions of $\overline{\mathcal{S}}_\ell^{dl}$ have now zero as criticality number, excepting the sets formed by one critical cell, which have one as criticality number.
- **[Updating initial dual AT-partition].** For each critical cell $e_q^{d_q} \in \mathcal{H}_\ell^\phi$ $(1 \leq q \leq m)$, let us construct the region of the dual segmentation $\overline{\mathcal{S}}_\ell^{dl}(e_q^{d_q}) = \{e_q^{d_q}\} \bigcup_{c \in \partial(e_q^{d_q})} \overline{\mathcal{S}}_\ell^{pr}(c)$ of dimension $dim^{dl}(\mathcal{S}_\ell^{dl}(e_q^{d_q})) = (d_q - 1, d_q)$. After updating the regions of the partition corresponding to the critical cells, the rest of regions of $\overline{\mathcal{S}}_\ell^{dl}$ remain unaltered. The resulting partition describes at set level the desired dual AT-segmentation and it is denoted by $\mathcal{S}_\ell^{dl}$. Let us emphasize that the ranks (that is, the difference between the number of cells of C and the number of regions of the partition) of the primal and dual AT-partitions can be different. This is mainly due to the fact that, in general, there is no one-to-one relation between critical cells and regions of the primal or dual AT-segmentations.
- **[Dimension and Bounding Function].** The dimension of a region $R \in \mathcal{S}_\ell^{dl}$, having t-cells and, possibly $t-1$ cells is $dim^{dl}(R) = (t, t-1)$. Its bounding function is defined by $B^{dl}[\mathsf{C}](R, R') = \#\{c \in R : dms(c) = t \wedge B(c, R') = \sum_{c' \in R'} B(c, c') \neq 0\} \quad \forall R, R' \in \mathcal{S}_\ell^{dl}$, with $dim^{dl}(R) = (t, t-1)$ and $dim^{dl}(R') = (t+1, t)$ $(1 \leq t \leq n)$.

At the end of this process, we get a dual AT-segmentation $HS^{dl}(\mathsf{C}) = (\mathcal{S}_\ell^{dl}, B^{dl}[\mathsf{C}], dim^{dl})$.

Let us note that the connectivity graph of regions of $HS^{dl}(\mathsf{C})$ is not necessarily a tree.

We are now ready to build a second order AT-RIG associated with the primal and dual AT-segmentations. AT-RIGs measure all the relationships between two homology classes of dimension t and $t+1$, $\forall 0 \leq t \leq n$. Let us write in pseudocode the construction of the second order primal AT-RIG (see Algorithm 2). The construction of the dual one is completely analogous.

Finally, the second order AT-RIG $G_1(AT(\mathsf{C}))$ is the graph whose nodes are the different homology classes (represented by their corresponding critical cell) and whose edges are those belonging to both primal and dual AT-RIGs.

4 Operations with AT-Segmentations

Given a primal (or dual) AT-segmentation, it is possible to create a new one changing only the participation of two cells. This operation is called *crack transport* and is exhaustively used in the parallel methods for computing homology information designed in [38].

Algorithm 2. [Second order Primal AT-RIG]

Input:

- an AT-model $(C, \partial_\ell, \phi_\ell, dms)$ and a combinatorial basis (set of *critical cells*) ordered by increasing dimension $\{e_1^{d_1}, \ldots, e_m^{d_m}\}$ (with $dms(e_q^{d_q}) = d_q$, $1 \leq q \leq m$) for the homology $H(\mathsf{C}, \phi)$.
- a primal AT-segmentation $HS^{pr}(\mathsf{C}) = (\mathcal{S}_\ell^{pr}, B^{pr}[\mathsf{C}], dim^{pr})$

for $i = 1$ to m **do**
  $v_i \leftarrow e_i^{d_i}$; ▷ the nodes of the RIG are the critical cells
  $N(v_i) \leftarrow \emptyset$ ▷ The set of all the neighbors of the region of the primal AT-segmentation containing v_i
  $N_s(v_i) \leftarrow \emptyset$ ▷ the set of neighbors of v_i in the second order AT-RIG
  for $j = 1$ to i **do**
    if $B^{pr}[\mathsf{C}](\mathcal{S}_\ell^{pr}(v_j), \mathcal{S}_\ell^{pr}(v_i)) \neq 0$ **then**
      $N(v_i) \leftarrow N(v_i) \cup \{v_j\}$;
      if $B^{pr}[\mathsf{C}](\mathcal{S}_\ell^{pr}(v_j), \mathcal{S}_\ell^{pr}(v_i)) = \#\{d_i - cells \in \mathcal{S}_\ell^{pr}(v_i)\}$ **then**
        $N_s(v_i) \leftarrow N_s(v_i) \cup \{v_j\}$;
        $B_{rig}^{pr}[\mathsf{C}](v_j, v_i) \leftarrow 1$;
    else
      $B_{rig}^{pr}[\mathsf{C}](v_j, v_i) \leftarrow 0$

Output: The region-incidence-graph $G_1^{pr}(AT(\mathsf{C}))$ associated to the abstract cell complex $(\{e_1^{d_1}, \ldots, e_m^{d_m}\}, B_{rig}^{pr}[\mathsf{C}], dms)$.

Algorithm 3 shows the admissible Crack Transport Algorithm. Crack transports can be used for AT-segmentation parallel computation.

Algorithm 3. [Admissible Crack Transport Algorithm].

Let $\mathcal{HS}(\mathcal{C})$ be a primal AT-segmentation of a geometric cell complex C. Let $\mathcal{R}_1$ and $\mathcal{R}_2$ be two regions of dimension $(k-1, k)$ and $(k, k+1)$ respectively, and $\mathbf{c} \in \mathcal{R}_1$ and $\mathbf{c}' \in \mathcal{R}_2$ be two k-cells. Let us denote by $\mathcal{HS}\tilde{(}\mathcal{C})$ the segmentation $\mathcal{HS} \setminus \{\mathbf{c}, \mathbf{c}'\}$. The new segmentation $[\mathbf{c} \leftrightarrow \mathbf{c}']\mathcal{HS}(\mathcal{C})$ resulting from the initial one, assigning $\mathbf{c}$ to $\mathcal{R}_2$ and $\mathbf{c}'$ to $\mathcal{R}_1$ is a new primal AT-segmentation if (a) $\mathbf{c}$ is incident to $\mathcal{R}_2$, $\mathbf{c}'$ is incident to $\mathcal{R}_1$;(b) there is at least a pair (S_1, S_2) of regions of $\mathcal{HS}\tilde{(}\mathcal{C})$ with $S_1 \subset \mathcal{R}_1$ $(dim^{pr}(S_1) = (k-1, k))$ and $S_2 \subset \mathcal{R}_2$ $(dim^{pr}(S-2) = (k, k+1))$, satisfying that:

- $\#(S_1 \cap \partial\mathbf{c}) = 1$ and $\#(S_1 \cap \partial\mathbf{c}') = 1$;
- $\#(S_2 \cap \delta\mathbf{c}) = 1$ and $\#(S_2 \cap \delta\mathbf{c}') = 1$;
- $B^{pr}[C](S_1, S_2) > 1$.

In Fig. 2, an internal (within the ROI) crack transport defined as an admissible interchange of cells between "connected" homological regions of the AT-segmentation of Fig. 1 is shown.

Another example of application of crack transport is shown in Fig. 3.

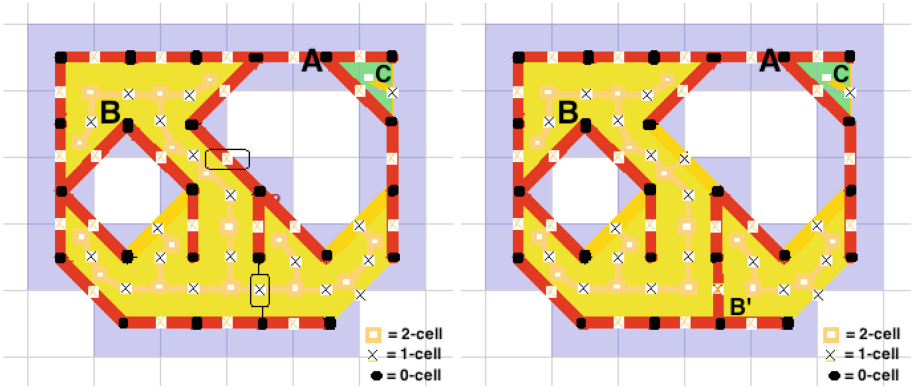

Fig. 2. (Left) AT-segmentation of Fig. 1. 1-cells involved in the internal crack transport are surrounded by black closed curves; (Right) Result of the crack transport. There are now three 1–2 regions B, B', C being the first two ones homologically essentials ($\beta^B = 1 = \beta^{B'}$). Both AT-segmentations present the same second order AT-RIG: a tree with three hole-nodes $(\alpha^0, \beta^1, \gamma^1)$, connecting α^0 with β^1 and γ^1.

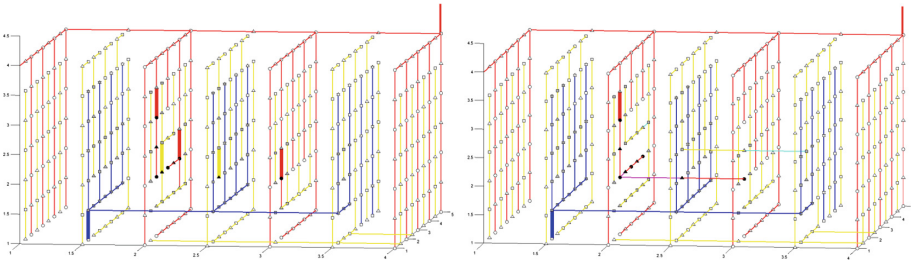

Fig. 3. A ROI composed of three segments parallel to the axis (a total of 5 black voxels). Points represent 0-cells (voxels), triangles 1-cells, squares 2-cells and stars 3-cells. Two AT-segmentations of the whole image that embeds the ROI are drawn. The AT-segmentation on the right is the result of several crack transport operations on the AT-segmentation on the left. Obviously, both have the same trivial AT-RIG: a trivial tree composed by one node (0-dimensional homology class of the image)

5 AT-RIG: Homological Tool or Topological Invariant?

The proof of homology and homotopy invariance of the AT-RIG is an issue out of the scope of this paper. The first part of this section is employed in supporting the thesis that the AT-RIG notion allows us to discriminate two non homologically equivalent objects having the same Betti numbers. Different instances (configurations spheres with handles, Menger sponges, torus, double torus, etc) are successfully examined with specific AT-segmentations. We only show here the example of AT-segmentations of simple cellular versions of the torus and the sphere with two handles.

On the other hand, we have only implemented software that calculates AT-segmentations (based on AT-models) but not AT-RIGs. Due to this reason, we expand the second part of this section to evaluate AT-segmentations of digital objects with known homology.

Given a torus (see Fig. 4), Fig. 5(a) shows a primal AT-segmentation, Fig. 5(b) an associated dual AT-segmentation, Fig. 6(a) its primal AT-RIG and Fig. 6(b) its dual AT-RIG.

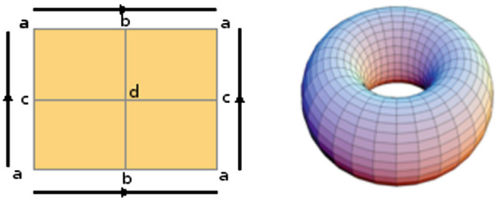

Fig. 4. Torus identification space

(a) Primal segmentation (b) Dual segmentation

Fig. 5. Torus primal and dual segmentations

In Fig. 7, given a cell model of a sphere with two handles, we provide a primal AT-segmentation Fig. 7(a), an associated dual AT-segmentation Fig. 7(b), its primal AT-RIG Fig. 8(a) and its dual AT-RIG Fig. 8(b).

Figure 9 shows an example of partition of a primal AT-segmentation of the Menger Sponge of recursion depth 2 [29], computed from an AT-model. The left side shows a Menger sponge with 400 0-cells, 1224 1-cells, 1056 2-cells and 312 3-cells. On the right side, a primal AT-partition is shown. The segmentation region of dimension $(0, 1)$ is shown in red. The regions of dimension $(1, 2)$ and $(2, 3)$ are shown in yellow and blue respectively. The second order primal AT-RIG is a star-type tree having as center the 0-dimensional homology generator (red region) and as leafs the 1-dimensional 81 homology classes (yellow regions R with $crt(R) > 0$). The blue regions do not appear in the second order primal AT-RIG due to the fact that their criticality number is zero. A similar example is shown in the lower part of Fig. 9 with a double torus. This example is composed by 714 0-cells, 1728 1-cells, 1280 2-cells and 268 3-cells. The second order primal AT-RIG

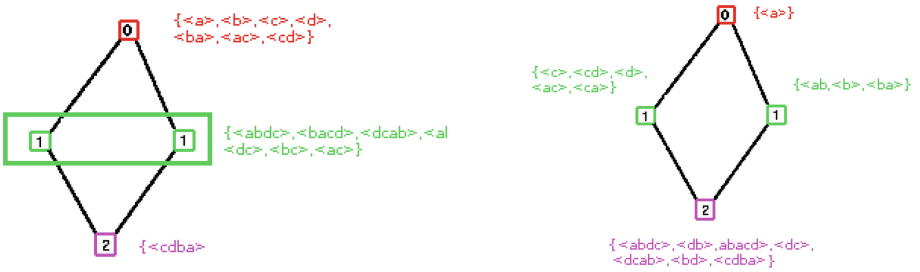

(a) Primal AT-RIG (b) Dual AT-RIG

Fig. 6. AT-RIGs for a torus

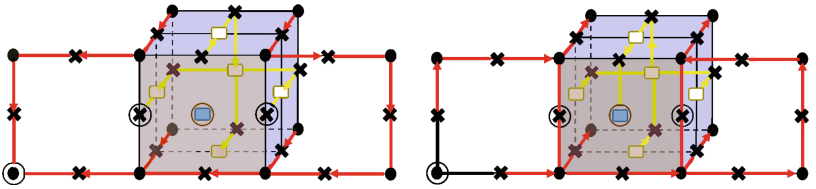

(a) Primal segmentation (b) Dual segmentation

Fig. 7. AT-segmentations for a sphere with two handles

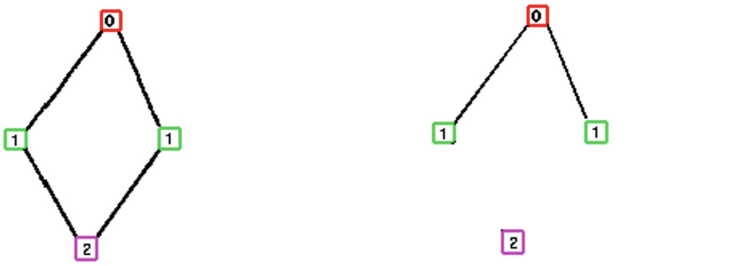

(a) Primal AT-RIG (b) Dual AT-RIG

Fig. 8. AT-RIGs for a sphere with two handles

for this example has a 0-dimensional homology generator (red region) connected to 4 1-dimensional homology classes (yellow regions R with $crt(R) > 0$) and all of them connected to a single 2-dimensional homology class representing the cavities (blue region R with $crt(R) > 0$).

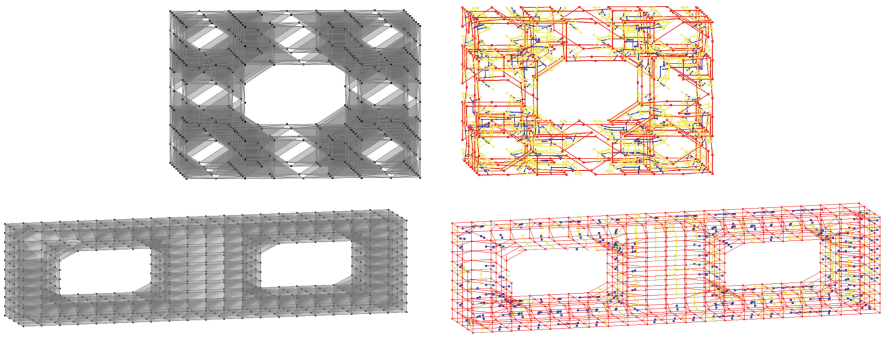

Fig. 9. (Left) A Menger Sponge of recursion depth 2 and a double torus (Right) Result of their respective primal AT-partitions, where the region of dimension $(0, 1)$ is colored in red, $(1, 2)$-regions in yellow and $(2, 3)$ regions in blue. (Color figure online)

6 Conclusions

In this paper, a new topological tool, called second order AT-RIG, for distinguishing cell complexes beyond Betti numbers or Euler characteristic is algorithmically designed. This tool allows to discover relationships between homology classes of dimension differing in one. The concise experimentation carried out supports the hypothesis that the AT-RIG is a well-defined notion and that these relations are "up to homology". To theoretically prove these results would suppose a true revolution in the field of the topological representation. Anyway, negative answers would still mean a step forward because we have a useful topological tool properly working within an AT-model context.

References

1. Alexandroff, P.S.: Combinatorial Topology. Dover, New York (1998)
2. Ayala, R., Domínguez, E., Francés, A.R., Quintero, A.: Homotopy in digital spaces. In: Borgefors, G., Nyström, I., di Baja, G.S. (eds.) DGCI 2000. LNCS, vol. 1953, pp. 3–14. Springer, Heidelberg (2000). https://doi.org/10.1007/3-540-44438-6_1
3. Boykov, Y.Y., Jolly, M.P.: Interactive graph cuts for optimal boundary and region segmentation of objects in ND images. In: Proceedings of Eighth IEEE International Conference on Computer Vision, vol. 1, pp. 105–112 (2001)
4. Cadek, M., Krcal, M., Matousek, J., Vokrinek, L., Wagner, U.: Polynomial-time computation of homotopy groups and Postnikov systems in fixed dimension. SIAM J. Comput. **43**(5), 1728–1780 (2014)
5. Carr, H.A., Weber, G.H., Sewell, C.M., Ahrens, J.P.: Parallel peak pruning for scalable SMP contour tree computation. In: IEEE 6th Symposium on Large Data Analysis and Visualization (LDAV), pp. 75–84 (2016)
6. Couprie, M., Bertrand, G.: Asymmetric parallel 3D thinning scheme and algorithms based on isthmuses. Pattern Recogn. Lett. **76**, 22–31 (2016)
7. Delfinado, C.J.A., Edelsbrunner, H.: An incremental algorithm for Betti numbers of simplicial complexes on the 3-sphere. Comput. Aided Geom. Des. **12**(7), 771–784 (1995)

8. Díaz-del-Río, F., Real, P., Onchis, D.: A parallel homological spanning forest framework for 2D topological image analysis. Pattern Recogn. Lett. **83**, 49–58 (2016)
9. De Floriani, L., Mesmoudi, M.M., Morando, F., Puppo, E.: Decomposing non-manifold objects in arbitrary dimensions. Graph. Models **65**(1), 2–22 (2003)
10. Dumas, J.G., Saunders, B.D., Villard, G.: On efficient sparse integer matrix Smith normal form computations. J. Symbol. Comput. **32**(1), 71–99 (2001)
11. Eilenberg, S., Mac Lane, S.: On the groups $H(\pi, n)$, II: methods of computation. Ann. Math. **60**, 49–139 (1954)
12. Forman, R.: Morse theory for cell complexes. Adv. Math. **134**, 90–145 (1998)
13. Hilaga, M., Shinagawa, Y., Kohmura, T., Kunii, T.L.: Topology matching for fully automatic similarity estimation of 3D shapes. In: Proceedings of the 28th Annual Conference on Computer Graphics and Interactive Techniques, pp. 203–212. ACM (2001)
14. De Floriani, L., Fugacci, U., Iuricich, F.: Homological shape analysis through discrete morse theory. In: Breuß, M., Bruckstein, A., Maragos, P., Wuhrer, S. (eds.) Perspectives in Shape Analysis. MV, pp. 187–209. Springer, Cham (2016). https://doi.org/10.1007/978-3-319-24726-7_9
15. Dumas, J.G., Heckenbach, F., Saunders, D., Welker, V.: Computing simplicial homology based on efficient Smith normal form algorithms. In: Joswig, M., Takayama, N. (eds.) Algebra, Geometry and Software Systems, pp. 177–206. Springer, Heidelberg (2003). https://doi.org/10.1007/978-3-662-05148-1_10
16. Fiorio, C.: A topologically consistent representation for image analysis: the frontiers topological graph. In: Miguet, S., Montanvert, A., Ubéda, S. (eds.) DGCI 1996. LNCS, vol. 1176, pp. 151–162. Springer, Heidelberg (1996). https://doi.org/10.1007/3-540-62005-2_13
17. González-Díaz, R., Real, P.: On the cohomology of 3D digital images. Discret. Appl. Math. **147**(2), 245–263 (2005)
18. González-Díaz, R., Jiménez, M.J., Medrano, B., Real, P.: Chain homotopies for object topological representations. Discret. Appl. Math. **157**(3), 490–499 (2009)
19. Gonzalez-Lorenzo, A., Bac, A., Mari, J.L., Real, P.: Allowing cycles in discrete Morse theory. Topol. Appl. **228**, 1–35 (2017)
20. Günther, D., Reininghaus, J., Wagner, H., Hotz, I.: Efficient computation of 3D Morse-Smale complexes and persistent homology using discrete Morse theory. Vis. Comput. **28**(10), 959–969 (2012)
21. Haarmann, J., Murphy, M.P., Peters, C.S., Staecker, P.C.: Homotopy equivalence in finite digital images. J. Math. Imaging Vis. **53**(3), 288–302 (2015)
22. Harker, S., Mischaikow, K., Mrozek, M., Nanda, V.: Discrete Morse theoretic algorithms for computing homology of complexes and maps. Found. Comput. Math. **14**(1), 151–184 (2014)
23. Hurewicz, W.: Homology and homotopy theory. In: Proceedings of the International Mathematical Congress, p. 344 (1950)
24. Klette, R.: Cell complexes through time. In: International Symposium on Optical Science and Technology, pp. 134–145. International Society for Optics and Photonics (2000)
25. Kong, T.Y., Rosenfeld, A.: Topological Algorithms for Digital Image Processing, vol. 19. Elsevier, Amsterdam (1996)
26. Kovalevsky, V.: Algorithms in digital geometry based on cellular topology. In: Klette, R., Žunić, J. (eds.) IWCIA 2004. LNCS, vol. 3322, pp. 366–393. Springer, Heidelberg (2004). https://doi.org/10.1007/978-3-540-30503-3_27
27. Lefschetz, S.: Algebraic Topology, American Mathematical Society Colloquium Publications, vol. 27. American Mathematical Society, New York (1942)

28. Lienhardt, P.: Topological models for boundary representation: a comparison with n-dimensional generalized maps. Comput. Aided Des. **23**(1), 59–82 (1991)
29. Menger, K.: Allgemeine Räume und Cartesische Räume, Teil I, Amsterdam, pp. 476–482 (1926)
30. Molina-Abril, H., Real, P., Nakamura, A., Klette, R.: Connectivity calculus of fractal polyhedrons. Pattern Recogn. **48**(4), 1150–1160 (2015)
31. Molina-Abril, H., Real, P.: Homological spanning forest framework for 2D image analysis. Ann. Math. Artif. Intell. **64**, 1–25 (2012)
32. Molina-Abril, H., Real, P.: Homological optimality in Discrete Morse Theory through chain homotopies. Pattern Recogn. Lett. **11**, 1501–1506 (2012)
33. Munkres, J.R.: Elements of Algebraic Topology. Addison-Wesley, Boston (1984)
34. Palmieri, J.H: Sage Module: Algebraic-Topological Model for a Cell Complex (2015). http://doc.sagemath.org/
35. Pilarczyk, P., Real, P.: Computation of cubical homology, cohomology and (co)homological operations via chain contractions. Adv. Comput. Math. **41**(1), 253–275 (2015)
36. Pudney, C.: Distance-ordered homotopic thinning: a skeletonization algorithm for 3D digital images. Comput. Vis. Image Underst. **72**(3), 404–413 (1998)
37. Real, P., Molina-Abril, H., Gonzalez-Lorenzo, A., Bac, A., Mari, J.L.: Searching combinatorial optimality using graph-based homology information. Appl. Algebra Eng. Commun. Comput. **26**(1–2), 103–120 (2015)
38. Real, P., Diaz-del-Rio, F., Onchis, D.: Toward parallel computation of dense homotopy skeletons for nD digital objects. In: Brimkov, V.E., Barneva, R.P. (eds.) IWCIA 2017. LNCS, vol. 10256, pp. 142–155. Springer, Cham (2017). https://doi.org/10.1007/978-3-319-59108-7_12
39. Romero, A., Rubio, J., Sergeraert, F.: Effective homology of filtered digital images. Pattern Recogn. Lett. **83**, 23–31 (2016)
40. Robins, V., Wood, P.J., Sheppard, A.P.: Theory and algorithms for constructing discrete Morse complexes from grayscale digital images. IEEE Trans. Pattern Anal. Mach. Intell. **33**(8), 1646–1658 (2011)
41. Saha, P.K., Borgefors, G., di Baja, G.S.: A survey on skeletonization algorithms and their applications. Pattern Recogn. Lett. **76**, 3–12 (2016)